Supplement of Atmos. Chem. Phys., 25, 15593–15611, 2025
https://doi.org/10.5194/acp-25-15593-2025-supplement

Atmospheric Chemistry and Physics
Open Access

Supplement of

Local-scale inversion of agricultural ammonia emissions: a case study on Schiermonnikoog, the Netherlands

Simeng Li et al.

Correspondence to: Simeng Li (s.li@cml.leidenuniv.nl)

Table S1. Agricultural emission, sector id 6

Enteric fermentation	Cattle	
	Sheep	
	Swine	
	Other animals	
Manure management	Cattle	dairy
		non-dairy
	Sheep	
	Swine	
	Buffalo	
	Goats	
	Horses	
	Mules and asses	
	Poultry	
	Broilers	
	Turkeys	
	Other poultry	
	Other animals	
Inorganic N-fertilizers (includes also urea application)		
Animal manure applied to soils		
Sewage sludge applied to soils		
Other organic fertilisers applied to soils		
Urine and dung deposited by grazing animals		
Crop residues applied to soils		
Farm-level agricultural operations		
Off-farm storage, handling and transport of bulk agricultural pr		
Cultivated crops		
Use of pesticides		
Rice cultivation		
Field burning of agricultural residues		
Urea application		
Other		

Table S2. The statistics of the modeled and the measured meteorological parameters on a daily basis: 10 m wind components (U and V), precipitation, temperature, and pressure, including Pearson's correlation coefficient (r), root-mean-square error (RMSE). Note that the measurement of pressure is not available at Lauwersoog and Nieuw Beerta.

			LW	LS	EE	NB
2019	U(m/s)	r	0.99	0.98	0.99	0.99
		RMSE	0.53	0.83	0.47	0.58
	V(m/s)	r	0.98	0.99	0.97	0.97
		RMSE	0.54	0.79	0.63	0.76
	T(K)	r	1.00	0.99	1.00	1.00
		RMSE	0.59	0.86	0.62	0.62
	R(mm)	r	0.75	0.83	0.81	0.82
		RMSE	3.34	2.18	2.19	2.06
	P(hPa)	r	1.00		1.00	
		RMSE	1.43		1.81	
2022	U(m/s)	r	0.99	0.99	0.99	0.99
		RMSE	0.66	0.86	0.47	0.64
	V(m/s)	r	0.98	0.98	0.96	0.97
		RMSE	0.58	0.79	0.69	0.71
	T(K)	r	0.99	0.99	0.99	1.00
		RMSE	0.62	0.85	0.63	0.52
	R(mm)	r	0.80	0.87	0.84	0.77
		RMSE	2.89	2.36	2.30	2.64
	P(hPa)	r	1.00		1.00	
		RMSE	1.32		1.64	

The abbreviations correspond to the site names: Leeuwarden, Lauwersoog, Eelde, and Nieuw Beerta.

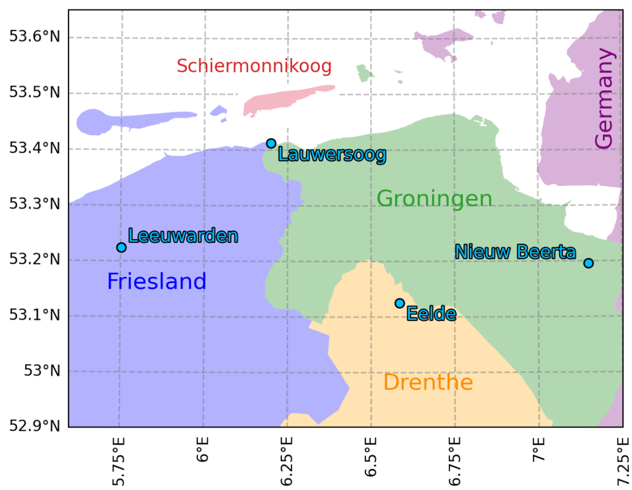

Figure S1. Meteorological measurement sites available for the validation (cyan circles): Leeuwarden, Lauwersoog, Eelde, and Nieuw Beerta.

(a) 2019

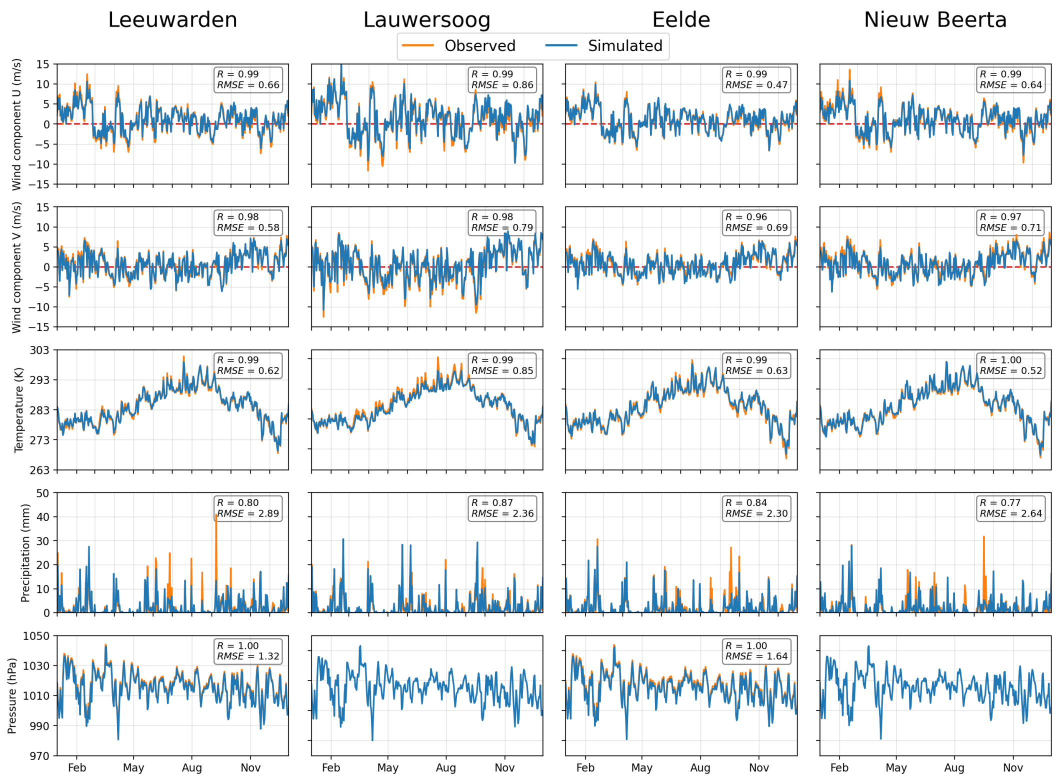

(b) 2022

Figure S2. Horizontal components of 10 m wind (U and V), precipitation, temperature, and pressure obtained from simulations and observations. The correlation coefficient R and the root-mean-square error RMSE are also presented.

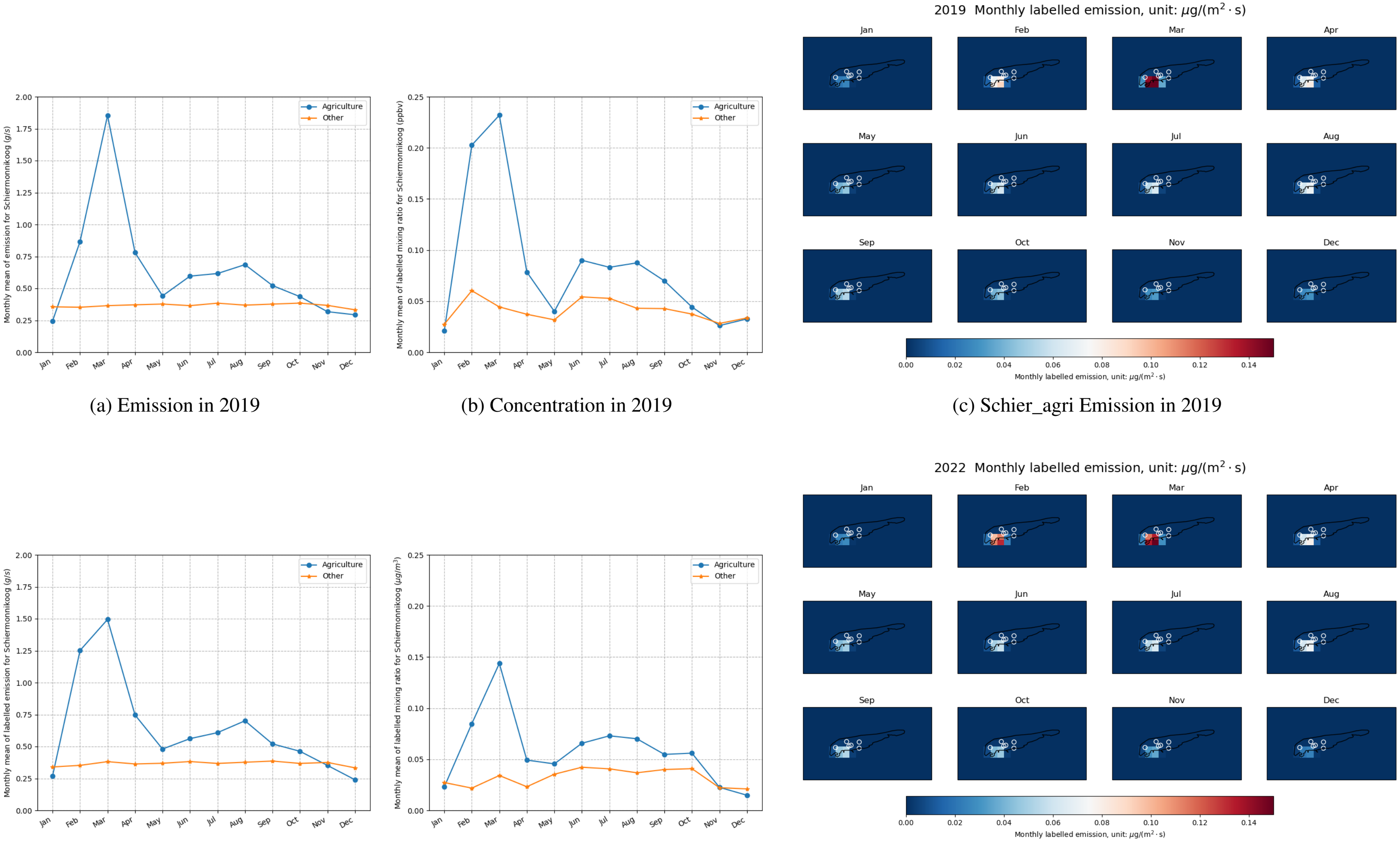

(a) Emission in 2019 (b) Concentration in 2019 (c) Schier_agri Emission in 2019

(d) Emission in 2022 (e) Concentration in 2022 (f) Schier_agri Emission in 2022

Figure S3. The monthly time profile for prior emissions and their contribution to local ammonia concentration on Schiermonnikoog in 2019 and 2022.

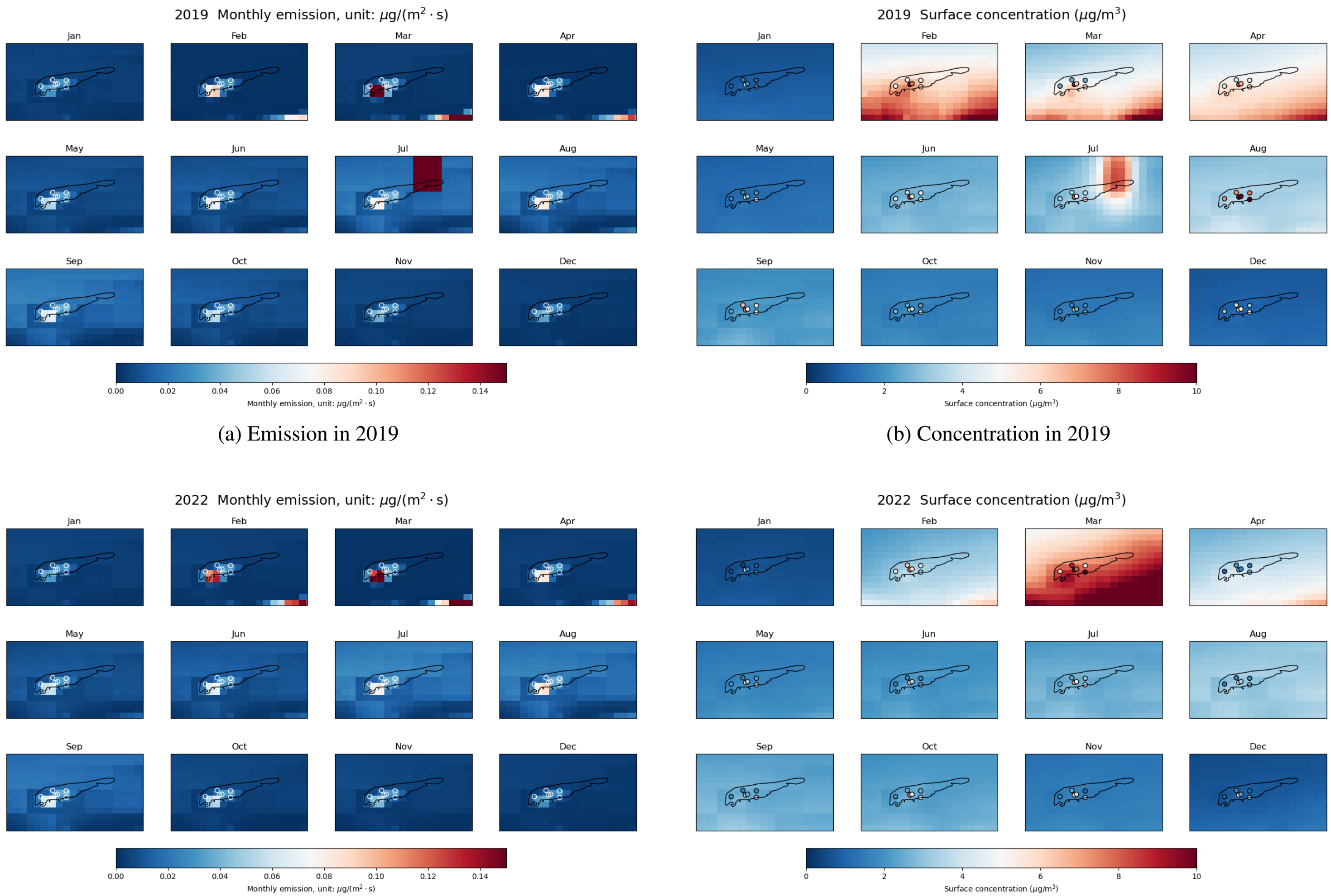

(a) Emission in 2019

(b) Concentration in 2019

(c) Emission in 2022

(d) Concentration in 2022

Figure S4. The monthly time profile for prior emissions and their contribution to local ammonia concentration on Schiermonnikoog in 2019 and 2022.

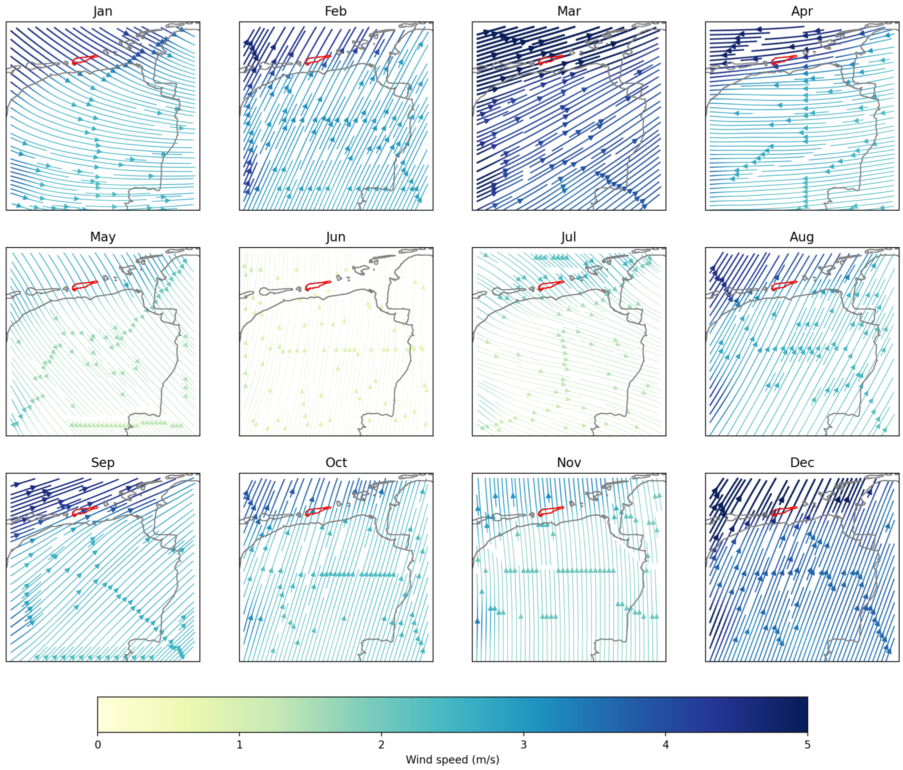

(a) 2019

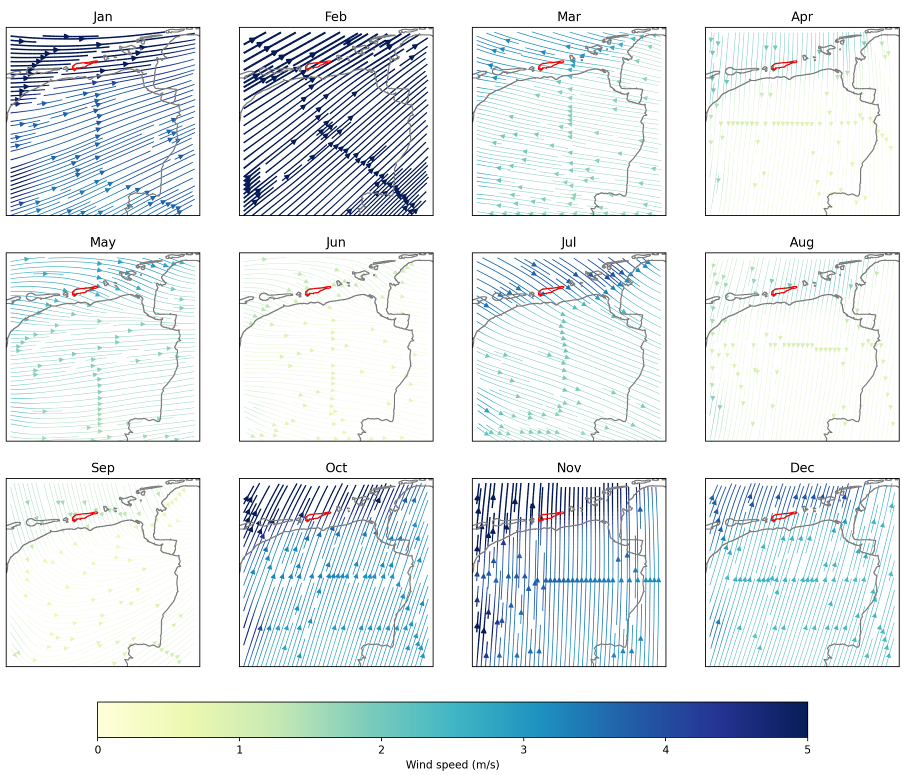

(b) 2022

Figure S5. Maps of wind field for 2019 (a) and 2022 (b).

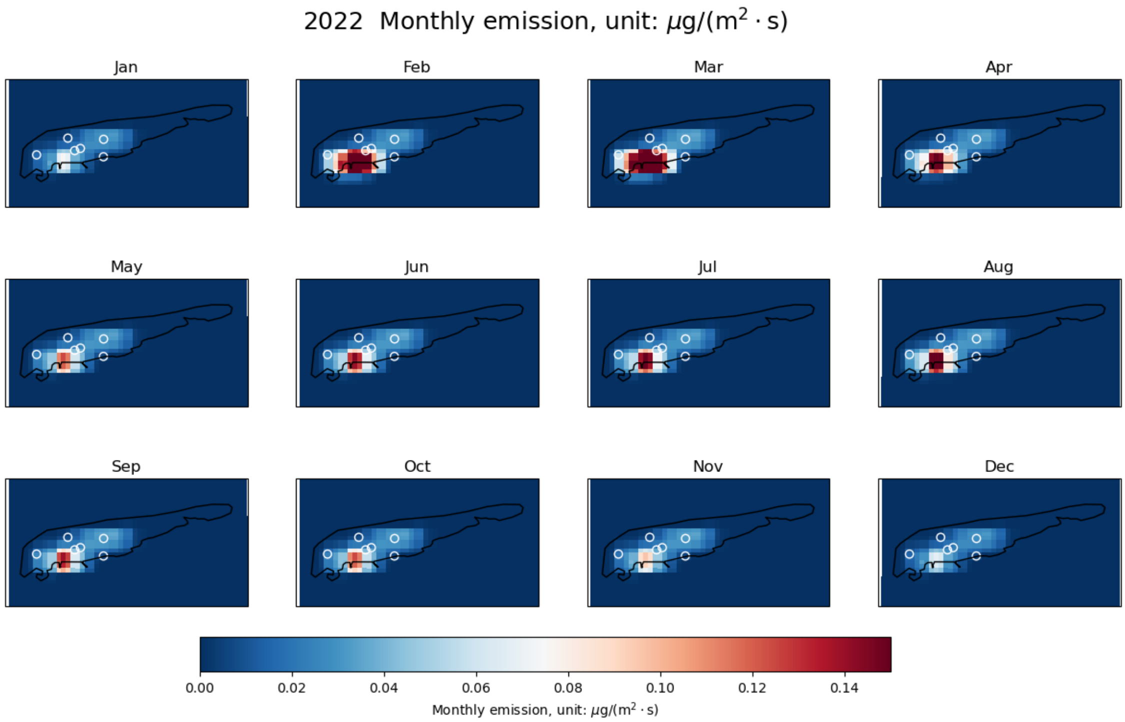

(a) Emssion

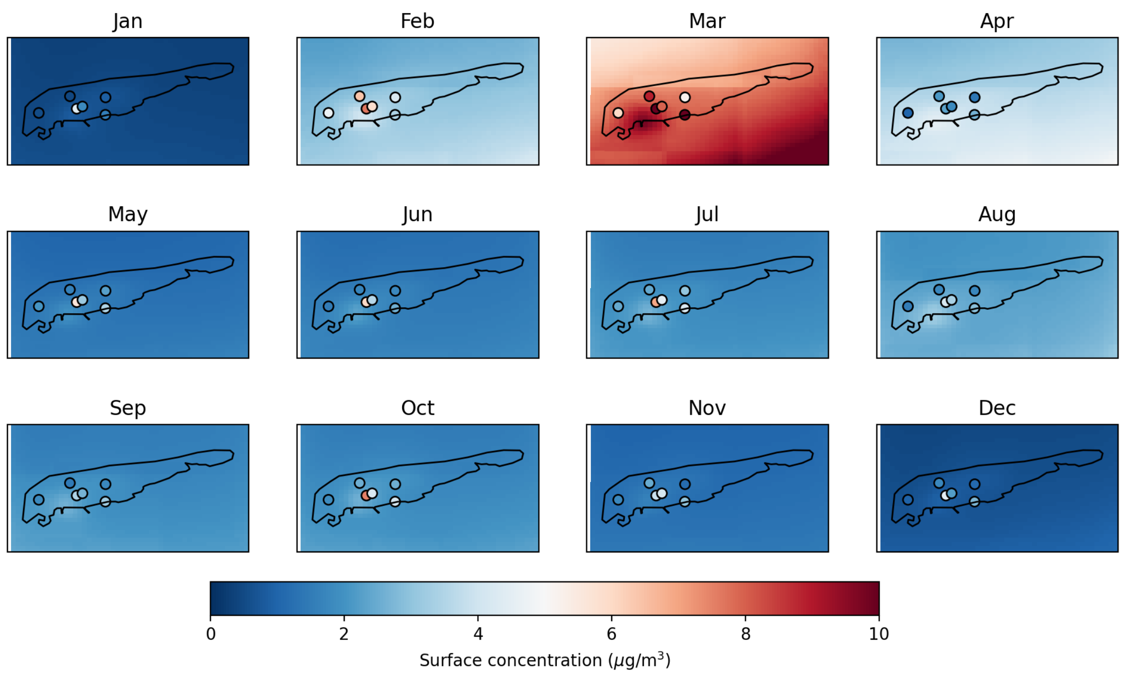

(b) Surface concentration

Figure S6. Maps of monthly emission (a) and simulated surface concentrations (b) on Schiermonnikoog for 2022 with the prior emission.

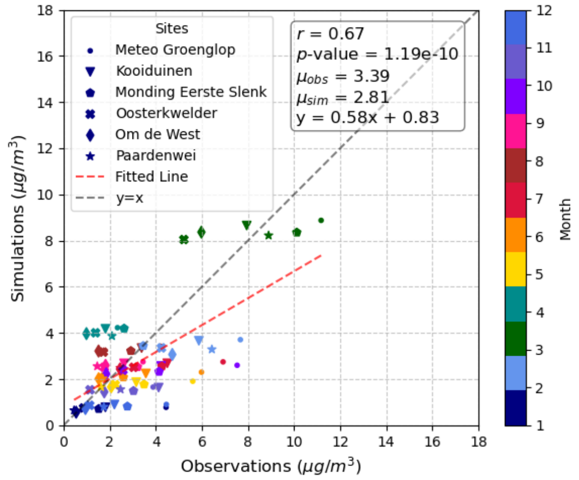

(a) Original resolution

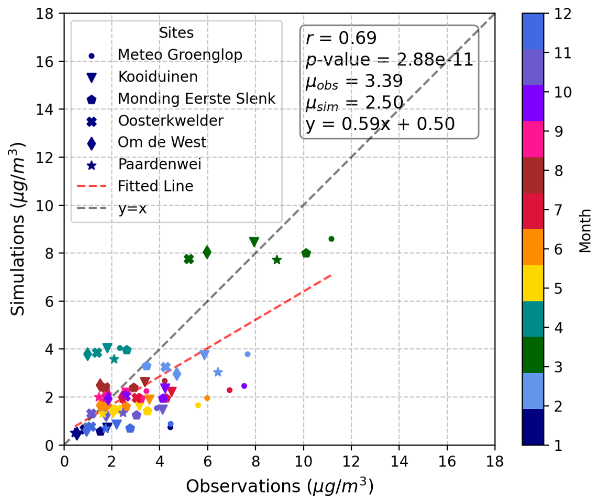

(b) 500 m × 500 m

Figure S7. The comparison of model and observation in the monthly average of 2022 on Schiermonnikoog with the prior emission.

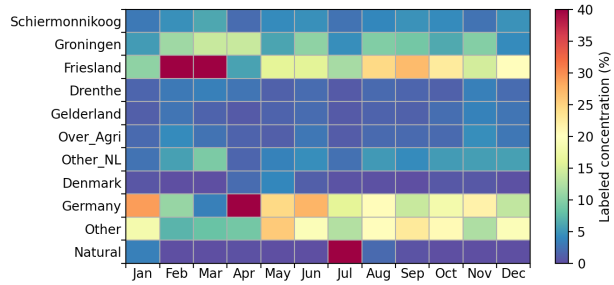

(a) Monthly results, 2019

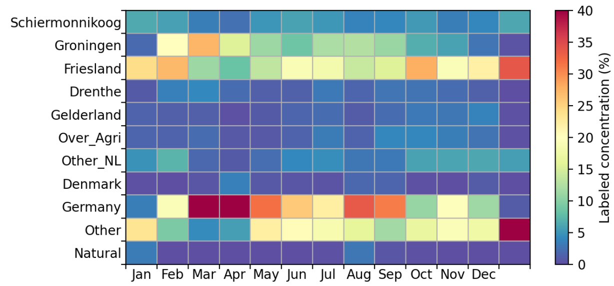

(b) Monthly results, 2022

Figure S8. The relative contributions of different sources to the surface concentration of Schiermonnikoog in 2019 (a) and 2022 (b) simulated by LOTOS-EUROS with the prior emission. Each row in the monthly figures shows the label's the contribution from only the agricultural sector.

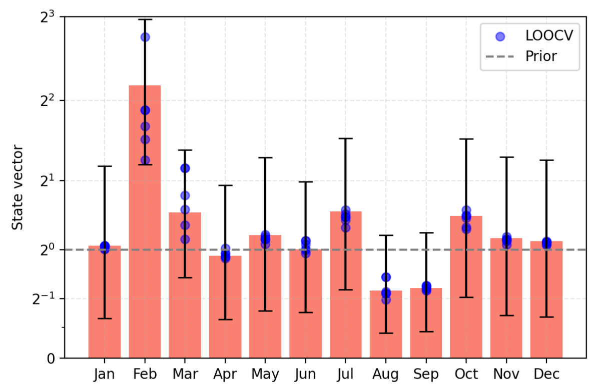

Figure S9. Results of MAN-derived yearly ammonia emission (a) and monthly ammonia emission (b) with credible intervals and the leave-one-out cross validation (LOOCV), derived from the posterior error covariance matrix $\hat{\mathbf{S}}$. The results shown in Figure (b) correspond to the 2022 inversion.

If we increase the measurements at the same sites, and then average those into one "super-observation" for that site, the total error could be reduced significantly and might be comparable to relatively high-quality measurement data. Assuming we have 6 sets of available MAN data at the very same site, then the total error should be, derived from Noordijk et al. (2020) Sect. 3.3:

$$s_{0\,\mathrm{tot}} = \left(\frac{s^2_{0\,\mathrm{MAN\ measuremnt}} + s^2_{0\,\mathrm{cal\ method}}}{6} \right)^{\frac{1}{2}} \approx 0.36 \mu\mathrm{g/m}^3 \tag{S1}$$

$$\mathrm{RSD}_{\mathrm{tot}} = \Bigg[\mathrm{RSD}^2_{\mathrm{MAN\ measuremnt}} + \frac{\mathrm{RSD}^2_{\mathrm{cal\ method}} + \mathrm{RSD}^2_{\mathrm{cal\ standard}}}{6} \Bigg]^{\frac{1}{2}} \approx 10\% \tag{S2}$$

While enhancing a single MAN site alone does not achieve the same performance as adding a single LML-like site (see Fig. S10a), substituting all six MAN sites on Schiermonnikoog with corresponding super-observations yields substantial improvements (Fig. S10b). In fact, this approach performs even better than the LML-like configuration in March and April. More details are provided in the Supplement.

References

Noordijk, H., Braam, M., Rutledge-Jonker, S., Hoogerbrugge, R., Stolk, A., and van Pul, W.: Performance of the MAN ammonia monitoring network in the Netherlands, Atmospheric Environment, 228, 117 400, https://doi.org/https://doi.org/10.1016/j.atmosenv.2020.117400, 2020.

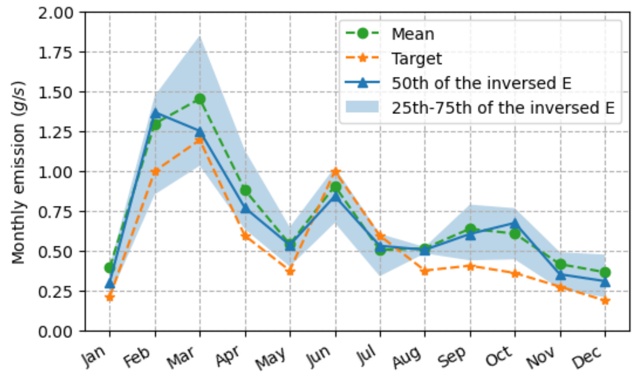

(a) One superobservation at Schiermonnikoog-Kooiduinen

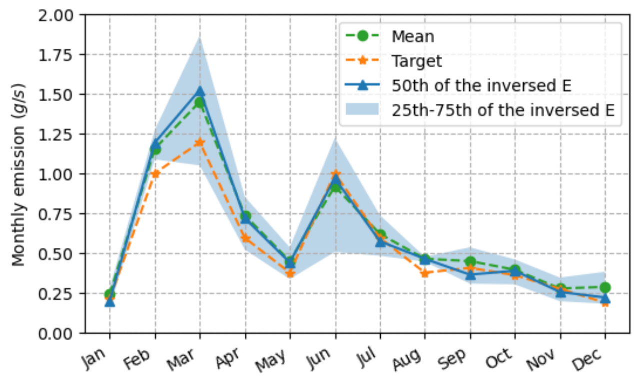

(b) Substitute all the 6 sites with superobservations

Figure S10. Posterior emission of the inversion with superobservations